SSRG International Journal of Electronics and Communication Engineering Volume 7 Issue 3, 35-41, March 2020
ISSN: 2348 – 8549 /doi:10.14445/23488549/IJECE-V7I3P106

Design of Barium Crown Glass Based Hollow Dual-Core Hexagon Pcf Filled With Selective Liquid

Divakar Kumar, Neha Kumari

Ph.D. Scholar, Research Scholar
Dept of Electronics and Communication
Sri Krishna University, Chhatarpur India-741302

Received Date: 20 February 2020
Revised Date: 28 March 2020
Accepted Date: 02 April 2020

Abstract
Two different dual hollow-core PCF structures are proposed, designed, and analyzed using Rsoft FEMSIM software. The first structure consists of a circular air hole, and the second structure consists of a square air hole. Silica glass is replaced by barium crown glass. The CS_2 is filled in the core, and the refractive index of CS_2 is 1.5956. Both square-shaped and circular-shaped hexagon lattice dual-core PCF made up of the same material. Low confinement loss, high birefringence as 1.093×10^{-3} for circular air holes and 8.49×10^{-3} for square air holes, Negative dispersion, effective refractive index, normalized frequency, effective area, and nonlinear coefficient are surveyed by varying the diameter of the air hole of cladding. Compare the parameters of both the designed PCF.

Keywords — *PCF, HCPCF, Photonic Band Gap, SPSM, QoS.*

I. INTRODUCTION

Photonic crystal fiber comprises of microstructure arrangement of air holes in the cladding region. Recently, PCF shows much curiosity due to the quality of bending easily without breaking (design flexibility) and distinctive light guiding properties. Two types of PCF: Index guiding and photonic band-gap PCF. Index guiding PCF consists of a core that is a solid fault area surrounded by an array of small air holes. Special properties of PCF such as flattened dispersion, low-loss, large effective area, decreases surface wave mode, and improved gain have attracted a lot of interest among the research work [1]. Photonic band-gap (PBG) fiber consisting core of giant hole surrounded by small array air holes. Such type of fiber is fabricated by using the stack and draw method. PBG fiber mitigates traditional optical fiber's various limitations in respect of loss, dispersion transmission spectrum, and nonlinearities. The guiding phenomenon of PCF depends upon the structure of the PCF and the geometrical parameters such as air hole diameter and pitch [2].

To get single-polarization single-mode operation functioning based on index-matching coupling, we initially select a high birefringence PCF. It is indicated that an undesired polarization state can be compressed by creating two cladding faults made up of a compact air hole inside its core. The proposed SPSM fiber shows a broad-spectrum range and possible application in domains of coherent communication. Polarization splitter is the most powerful equipment in optical communication and fiber optic sensing. Metal-filled square lattice dual-core PCF used as a broadband polarization beam splitter. The simulation results of dual-core PCF show coupling properties. The coupling properties depend on the designed parameters like pitch and air hole diameter. Such a unique category of polarization splitter could be mostly used in the passive optical network **[3,4,5].** Dispersion compensated fiber is used in long-distance communication to minimize the spreading of pulses. Dispersion compensation plays an important role in optical communication. Single-mode circular PCF is designed to analyzed effective dispersion, relative dispersion slope, bi-refringence, and confinement loss **[6].** Young Zhao et al. proposed a magnetic fluid-filled PCF.
Demonstrated the magnetic field guide light intensity in PCF analyses various properties such as effective refractive index, effective mode area as a function of wavelength and shows the correlation between the magnetic field and effective index **[7].** Vinod Parmar et al. reported a hollow-core PCF filled with gas. Gas-filled PCF is used to analyze the flow of gases. Gas-filled HC-PCF has wide applications, such as a gas sensor. Molecule diameter and molecular weight played a key role in the designing of gas-filled PCF **[8].** Hamed Saghaei et al. presented silica and chalcogenide-based three fiber structure. Linear and nonlinear characteristics of the PCF are obtained using the finite difference Eigenmode method. Varying the physical magnitude of the PCF, such as

by increasing the air hole diameter, the value of dispersion decreases **[9].**

Gas-filled hollow-core PCF proffer unrivaled chance to obtain several complicated nonlinear occurrences such as combined solution, single temporal solution, and solution dynamics. Raman solution pulses gas-filled hollow-core PCF was considering interference **[10].** Very low confinement loss, high dispersion coefficient are observed theoretically. Germanium doped rod is placed in the center of the PCF and measured various parameters **[11].**Microstructure air hole of dual-core PCF filled with selective liquid. Such type of PCF is used as a sensor. The liquid is easily inserted inside the air hole of PCF as compare to solid and gas. Liquid-filled PCF possesses high sensitivity. A dual-core octagonal PCF-based polarization splitter is used to calculate the effective index **[12, 13,14].**

In this paper, various optical properties as a function of wavelength of a carbon disulfide and barium crown glass-based PCFs are analyzed. The proposed two structures of hollow dual-core PCF consist of circular-shaped and square-shaped six air holes. Both structures are aligned in a hexagonal lattice. Section II describes the cross-sectional view of the model. Section III describes the numerical simulation. The Rsoft FEMSIM software is used for the simulation. Using Rsoft FEMSIM software, various properties of the proposed model, including confinement loss, birefringence nonlinearity, effective area, normalized frequency, are demonstrated.

II. PROPOSED PCF MODEL

The presented dual hollow-core PCF has been shown in Figures 1 and 2.

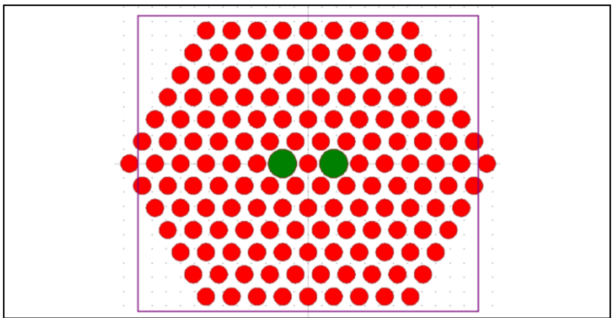

Figure 1. Structure of dual hollow-core circular air hole hexagon PCF.

The air holes are arranged in a hexagonal fashion. The proposed PCFs are constructed using constant pitch (Λ)= 1.8 μm, and the air hole diameter are 1.188, 1.224, 1.260, 1.296, and 1.332μm, respectively. Barium crown glass is used as background material, and carbon disulfide is filled in the PCF core. The circular-shaped air holes are arranged in a hexagon, as shown in figure 1. The diameter of the inner dual-core is 2μm, which is bigger than the cladding air holes. The square-shaped air holes are arranged in hexagon form, as shown in figure 2.

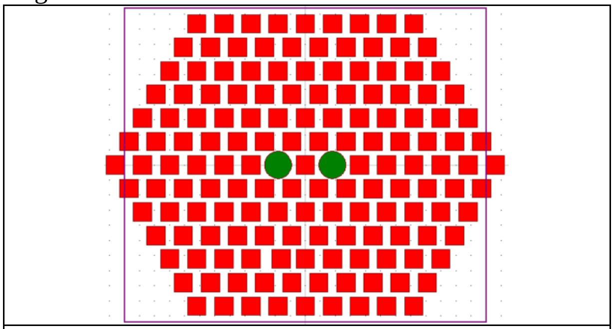

Figure 2. Structure of dual hollow-core square air hole hexagon PCF

In the square-shaped air holes hexagonal structure, the size of the inner dual-core is 1.8μm. The same materials are used in both the designed PCF. The same liquid is filled in the inner ring of both the PCF. The refractive index of the liquid is 1.5956and the refractive index of background material is 1.57.

Simulation results acutely indicate that the light in optical fiber is closely confined into the core region. The assigning of the electric field of both the designed PCF is shown in figure 3. The light is confined in both cores of the PCF. The designed dual-core PCF is used as a coupler. So, the details of the dual hollow-core designed PCF's power coupling efficiency are given by the intervention of the fiber core E_x and E_y guided modes.

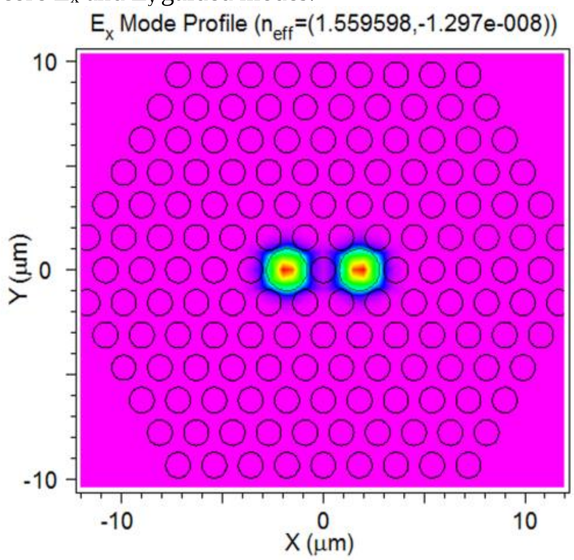

Fig:-3(a) Field distribution along with E_x mode of the first structure.

Fig. 3 Electric field distribution of hexagon hollow-core PCF (a) E_x mode of first structure made with circular air holes (b) E_y mode of first structure made with circular air holes (c) E_x mode of second structure made with square air holes (d) E_y mode of second structure made with square air holes.

Light is concentrated in the core of the two different hexagonal dual-core PCF. The E_x mode and E_y mode of the circular air hole hexagonal dual-core PCF is shown in figure 3(a) and 3(b).

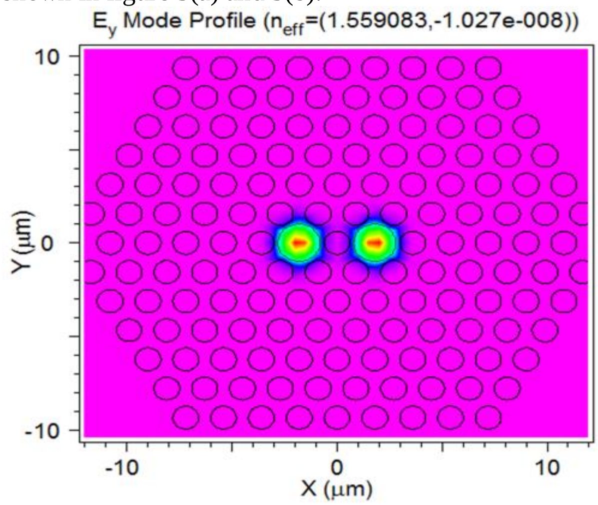

Fig3(b) Field distribution along with E_y mode of the first structure.

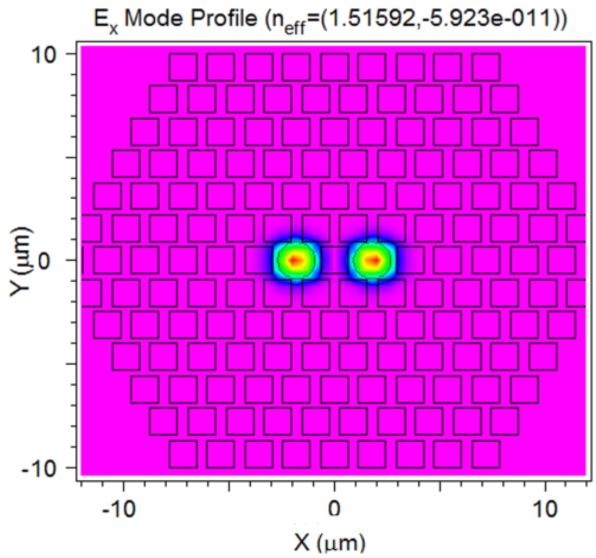

Fig:-3(c) Field distribution along with E_x mode of the second structure.

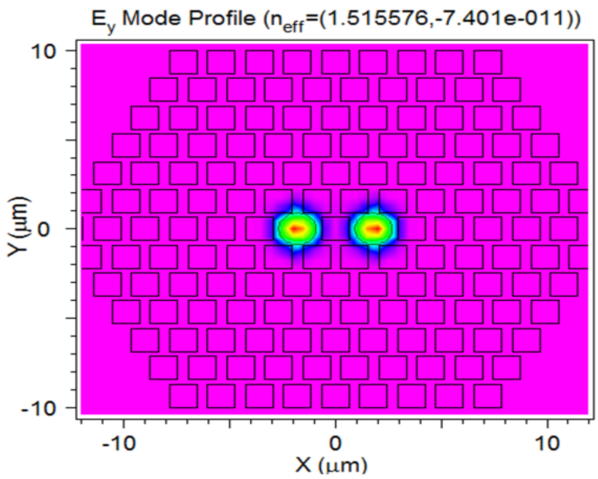

Fig:-3 (d) Field distribution along with E_y mode of the second structure.

In figure 3(c) and 3(d), the two different modes along E_x and E_y of the square air hole hexagonal dual-core PCF is demonstrated.

III. NUMERICAL CALCULATION OF THE FIBER

In this portion, the numerical computation of the designed PCF will be explained. Also, compare the result of the designed fiber. The effective refractive index is a main parameter of the PCF. Using Rsoft FEMSIM software, the effective refractive index (n_{eff}), for the designed PCF is calculated. The graph of effective refractive index as a concern of wavelength is shown in Figures 4and 5. The effective refractive index depends on the wavelength and light intensity.

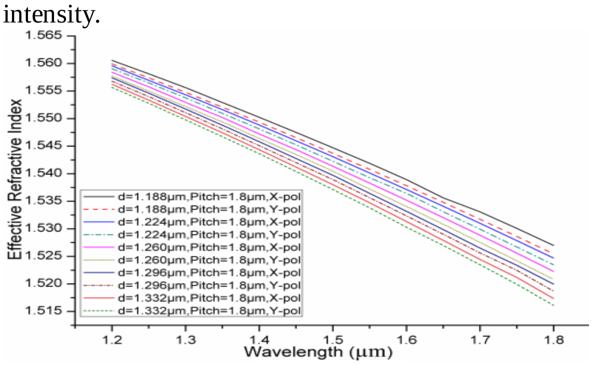

Fig.4 Effective refractive index of circular air hole PCF

Figure 4 shows the effective refractive index of circular air holes PCF as a function of wavelength for different diameters of the air holes and constant pitch.

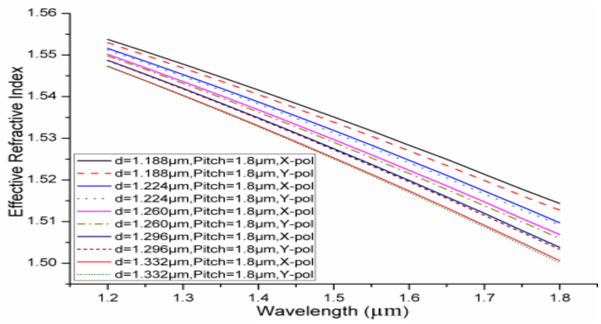

Fig.5. The effective refractive index of square air hole PCF

In Fig.5, the effective refractive index of square air hole PCF as a function of wavelength for different diameter of the air holes and constant pitch. From the graph 4 and 5 it is observed that as the wavelength increases the n_{eff} decreases.

From figure 5, it is observed when the diameter is 1.296 and 1.332; there is little difference between the value of n_{eff} along X and Y polarization.

The confinement loss(L_c) is one of the vital parameters of the PCF.By using the imaginary part of the n_{eff}, L_c for both the designed PCF can be calculated (1)**[15].**

$$L_c = 8.686 \; k_0 \; Im[n_{eff}]*10\text{^}6 \; dB/m \ldots\ldots\ldots\ldots\ldots\ldots (1)$$

Where k_0 is the wavenumber in free space and $Im[n_{eff}]$ is the imaginary part of the effective refractive index. Using equation 1, the numeric value of L_c was determined for two different types of designed PCF.

The graphs of the L_c for circular and square air holes are shown in Figures 6 and 7.

In figure 6, the confinement loss(Lc) first increases with wavelength increases and then decreases with an increase of wavelength.

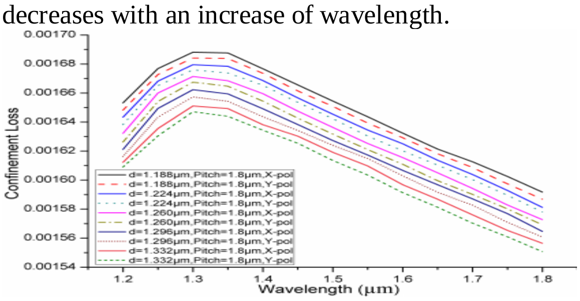

Fig.6. Confinement loss as function of wavelength of circular air hole for different diameter and constant pitch

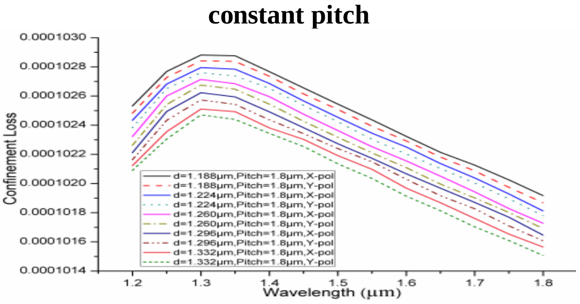

Fig.7 Confinement loss as a function of wavelength of square air hole for different diameter and constant pitch.

The graph of confinement loss in figure 7 also increases and then decreases with increases of wavelength. The nature of the L_c graph for both circular and square air holes is the same. But the hexagon dual hollow-core PCF made up of square air holes has lower confinement loss than the circular air hole. The value confinement loss of circular and square air hole PCF is along x and y axes are 1.61 $x10^{-3}$, 1.60 $x10^{-3}$dB/m and 1.021 $x10^{-4,}$ 1.020 x 10^{-4} dB/m respectively. By changing the diameter of air holes from 1.188-1.332, the numerical result of the confinement loss becomes smaller.

In the case of PCF, high birefringence can easily obtain as compared to conventional fiber. It depends on the structural parameter like the size of the microstructure air holes and the wavelength. The value of the effective refractive index is obtained by using the Rsoft FEMSIM software. With an effective refractive index, birefringence is obtained using the given formula (2)**[15].**

$$B = Re\,(n_{effx} - n_{effy})\ldots\ldots\ldots\ldots\ldots\ldots\ldots\ldots\ldots (2)$$

Where n_{effx}, n_{effy} represents an effective refractive index of x and y modes, and Re represents the effective refractive index's real part. The graph of birefringence is shown in figure 8.

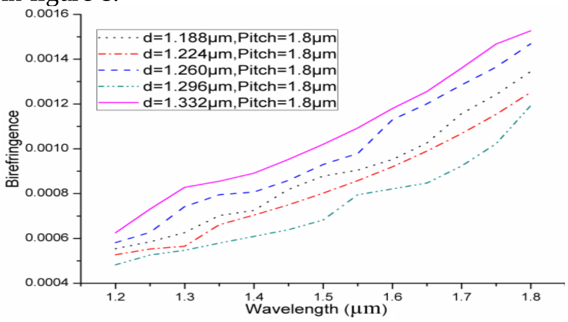

Fig.8. Bi-refringences of circular air holes hexagonal hollow dual-core PCF as a function of wavelength.

The birefringence curve of circular air hole hexagonal hollow dual-core PCF increases with wavelength, as shown in figure 8. The value of birefringence is high; when the diameters of the air holes are 1.332µm. Here the value of birefringence decreases as the diameter of the air hole becomes smaller.

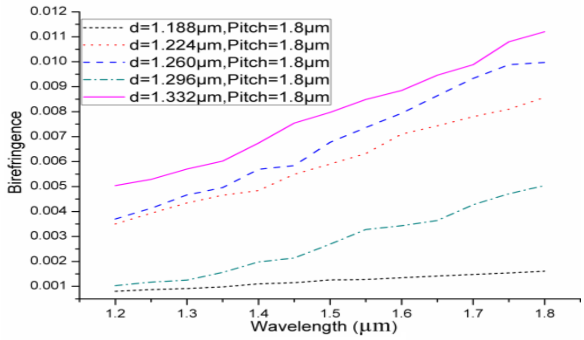

Fig.9. Birefringence of square air hole hexagonal hollow dual-core PCF as a function of wavelength.

The curve of birefringence for square air hole hexagonal dual-core PCF is shown in figure 9. The birefringence curve depends on the wavelength and the dimension of the air holes. It is seen in figure 9, the value of birefringence is high when the diameter is 1.332µm. The lowest value of birefringence is obtained when the diameter is 1.88µm. The birefringence is 1.093 x 10^{-3} for circular air holes hexagonal hollow dual-core PCF, and for square air holes hexagonal hollow dual-core PCF, the birefringence is 8.49 x 10^{-3} when the diameter of air holes is 1.332µm at 1.55µm wavelength.

Dispersion is an important parameter of optical fiber. In PCF, negative or zero dispersion can be obtained. The graph of dispersion of circular air holes hexagonal hollow-core PCF is shown in figure 10. The negative dispersion PCF is useful for long-distance communication because it minimized cross-talk or interference. Figure 10, a graph of dispersion is obtained from Rsoft FEMSIM software. Dispersion of PCF is wavelength-dependent and affected by several air holes. Circular air holes of hexagonal hollow dual-core PCF display negative dispersion, as shown in figure 10 given below. The green color line represents the dispersion curve.

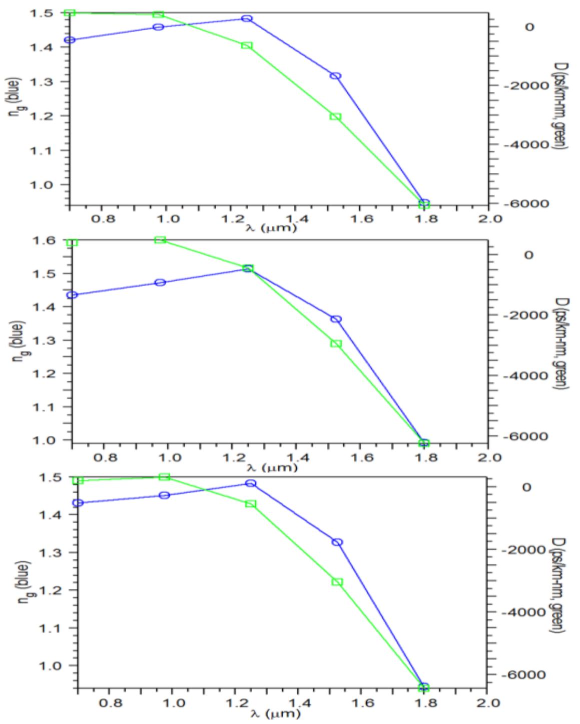

Fig.10 Dispersion graph of circular air holes of hollow dual-core PCF for five diameters of air holes, d = 1.188, 1.224, 1.260.

The total three graphs are obtained for five diameters at a constant pitch. The size of air holes is in micro-meter (µm). From the figure10, it is observed that the curve of dispersion first shows a straight line and then decreases smoothly. The graph of the dispersion of square air holes hexagonal hollow dual-core PCF is shown in figure 11.

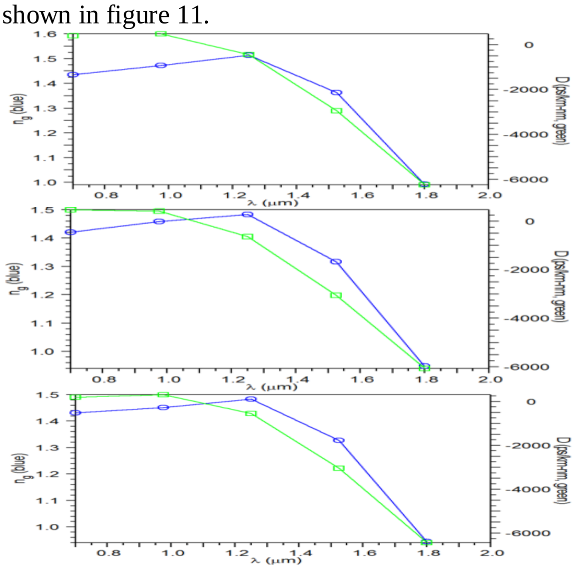

Fig. 11. dispersion curve of square air holes hexagonal hollow dual-core PCF for d = 1.188, 1.224, 1.260 µm and pitch is 1.8 µm as a function of wavelength.

The V_{eff} depends on the size of air holes arrangement in the cladding region, and it is calculated by using the following formula (3)**[16]**

$$\mathbf{Veff = 2\pi\ \rho\ /\ \lambda\ [sqrroot(n^2_{co} - n^2_{fsm})] \ldots\ldots\ldots\ldots\ldots\ldots (3)}$$

Where ρ represents the effective core radius, n^2_{co} and n^2_{fsm} denote the effective index of core and cladding, and λ is the wavelength in µm.

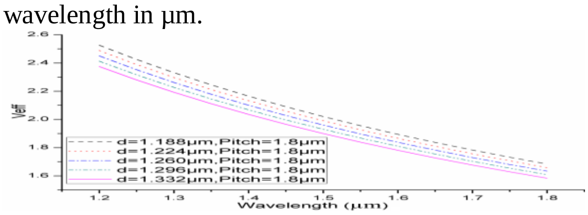

Fig.12. V_{eff} of circular air holes hexagonal hollow dual-core PCF

The value of normalized frequency is measured along with the 1.2-1.8µm wavelength range. The graph of V_{eff}(normalized frequency) of circular air holes is shown in figure 12. The curve of normalized frequency decreases slowly concerning wavelength. From figure 12, it is observed that the normalized frequency is 1.83874 at wavelength 1.55µm. The lowest value of normalized frequency is obtained when the diameter of air holes is 1.332µm. The highest value of normalized frequency is obtained when the air holes' diameter is smaller than 1.332µm.

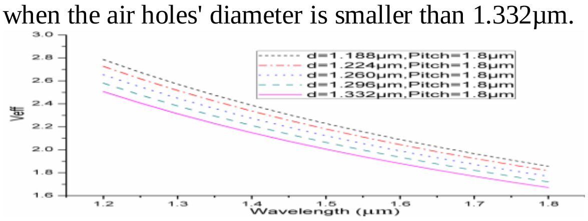

Fig.13. V_{eff} of square area holes hexagonal hollow dual-core PCF

. In figure 13, the normalized frequency of square air holes is shown. From figure 12 and 13, it is observed that the nature of curve of normalized frequency is same for both the structure. The normalized frequency is 1.94089 for square air holes at 1.55µm.

The graph of effective area for five different diameters of air holes is plotted. All the five curves for different diameters are merged, as shown in figure 14. The effective area depends upon the air holes, pitch, and wavelength. The effective area for PCF is calculated by using the given equation (4)[17].

$$\text{Aeff} = \pi[W_{PCF}]^2 \ldots\ldots\ldots\ldots\ldots\ldots\ldots\ldots\ldots\ldots\ldots\ldots\ldots\ldots\ldots\ldots\mathbf{(4)}$$

Where $[W_{PCF}]^2$ denotes the spot size.

The curve of effective area for the different diameters is closed to each other, and from graph 14, it is also analyzed that there is little variation in the value of A_{eff}. The graphs of A_{eff} of circular air holes are plotted as a function of wavelength by varying the diameter, as given in figure 14. At 1.55µm the A_{eff} is 30.59 µm^2 when the diameter is 1.332µm. The second graph of square air holes-based PCF is also plotted as a wavelength function, as shown in figure 15. A_{eff} is 15.68 μm^2 when the diameter is 1.332μm at 1.55μm wavelength. By comparing both the values of A_{eff} , it is found that the effective area of square air holes based PCF are less as compare to the circular air hole PCF.

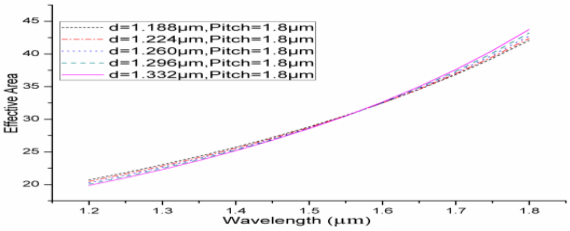

Fig. 14. the curve of effective area of circular air holes of hexagonal hollow dual-core PCF

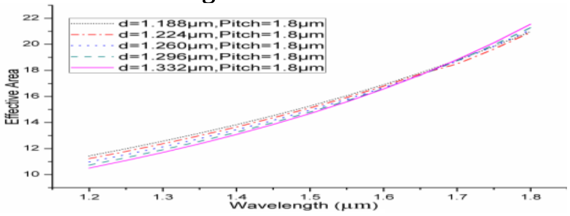

Fig.15. The curve of effective area of square air holes of hexagonal hollow dual-core PCF

From the figure 14 and 15, it is observed that both the graph having the same nature. In figure 14, the curve of A_{eff} coincides between the 1.55- 1.7 μm wavelength, but in figure 15, the coincide point shifted, and it lies between the 1.7-1.755 μm wavelength.

First, we need the value of $A_{eff,}$ and then we calculate the nonlinear coefficient of PCF. The nonlinear coefficient depends on the wavelength and effective area. ϒ denotes the nonlinear coefficient, and it is obtained as(5)**[18].**

ϒ= 2π/ λ(n2/ A_{eff})……………………………(5)

where 2π is constant, λ is wavelength in μm, and A_{eff} is the effective area measured in μm^2.

From figure 16, the nonlinear coefficient of circular-shaped air holes-based PCF decreases with an increase of wavelength.

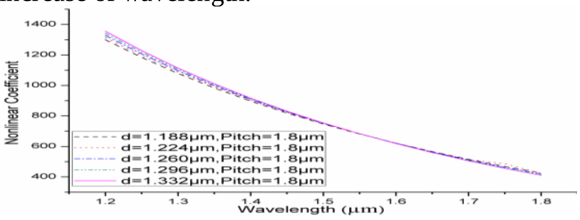

Fig. 16 Nonlinear coefficient vs. wavelength for constant pitch and d = 1.188, 1.224, 1.260, 1.296, and 1.332 μm.

The graph of the nonlinear coefficient of square air holes is shown in the figure.17 given below. The non-linear coefficient is 1336.745$w^{-1}km^{-1}$at1.55μm. The curve decreases with an increase of wavelength and also depends on the effective area.

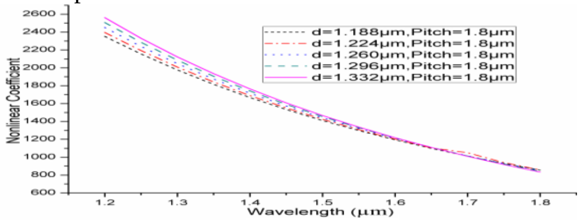

Fig.17 Graph of nonlinear coefficient of square air holes hexagon hollow dual-core PCF.

IV. CONCLUSION

Dual-core PCFs are presented in which two structures consist of the same number of air holes in the cladding region and the same pattern. The presented PCF are arranged in a hexagonal form, and the central dual-core is filled with carbon disulfide. The background material is barium crown glass. Using Rsoft FEMSIM software, the presented PCF is designed and simulated. It is found that square is holes-based PCF shows the better result as compare to circular air holes. Such a kind of PCF is used as a filter, coupler. This paper will help in the advancement and enhancement of optical fiber communication with better quality of services (QoS)in optical communication.

REFERENCES

[1] Ali Rostami and HadiSoofi, "*Correspondence Between Effective Mode Area and Dispersion Variations in Defected Core Photonic Crystal Fibers*," Journal of Lightwave Technology, vol.29, pp. 234-241, January 2011.

[2] Theis P. Hansen, JesBroeng, Christian Jakobsen, Guillaume Vienne, Harald R. Simonsen, Martin D. Nielsen, Peter M. W. Skovgaard, Jacob R. Folkenberg, Anders Bjarklev, "*Air-guiding photonic bandgap fibers: spectral properties, macrobending loss, and practical handling*", Journal of Lightwave Technology,vol.22,pp.11-15,2004.

[3] Sun Goo Lee, Sun Do Lim, Kwanil Lee, Sang Bae Lee, "*Single-polarization single-mode photonic crystal fiber based on index-matching coupling with a single silica material*," Optical fiber technology, vol. 17, pp. 36-40, October 2010.

[4] LinghongJianga,n, Yi Zhenga, LantianHoub, Kai Zhenga, JiyingPenga, XingtaoZhaob, "*An ultra-broadband polarization splitter based on square-lattice dual-core photonic crystal fiber with a gold wire*," Optics Communication, vol. 351, pp.50-56, April 2015.

[5] QiangXu, Miao Wang, Shebao Lin, Zhihuai Yang, Yani Zhang, Lei Zhang, Runcai Miao, "*A novel polarization splitter based on dual-core photonic crystal fibers*," Optik, vol. 127, pp. 10442-10449, August 2016.

[6] M.Mejbaul Haque, M.Shaifur Rahman, M.Samiul Habib, S.M.A Razzak, "*Design and characterization of single-mode circular PCF for broadband dispersion compensation*," Optik, vol.125, pp. 2608-2611, November 2013

[7] Yong Zhao, Yuyan Zhang, Qi Wang, RiqingLv, "*Optical sensing characteristics of the photonic crystal fiber filled with magnetic fluid*," Optik, vol. 125, pp.1829-1832, September 2013.

[8] Vinod Parmara, Randhir Bhatnagara, "*Analysis of gas flow dynamics in hollow-core photonic crystalfibre based gas cell*," Optik, vol. 125,pp. 3204-3208,December 2016.

[9] Hamed Saghaei, Vahid Heidarib, Majid Ebnali-Heidaric, Mohammad RouhollahYazdanib, "*A systematic study of linear and nonlinear properties of photonic crystal fibers*", Optik, vol.127, pp.11938-11947, September 2016.

[10] Thang Nguyen Manh, Thanh Thai Doan, "*A train of backward Raman soliton pulses in hollow-core photonic crystal fibres filled with hydrogen gas*", Optik, vol.127, pp.10259-10265, August 2016.

[11] Jui-Ming Hsu, Wen-Hao Zheng, Cheng-Ling Lee, Jing-ShyangHorng, "*Theoretical investigation of a dispersion compensating photonic crystal fiber with ultra-high dispersion coefficient and extremely low confinement loss*" , Photonics and nanostructures, vol.16, pp. 1-8, June 2015

[12] Rahul Kumar Gangwar, Vinod Kumar Singh, "*Refractive index sensor based on selectively liquid infiltrated dual core photonic crystal fibers*", Photonics and nanostructure, vol.2, pp. 5001-5007, March 2015.

[13] Qiang Liu, Shu-Guang Lin, Min Shi, "*FiberSagnac interferometer based on a liquid-filled photonic crystal fiber for temperature sensing*", Optics Communication, vol.381, pp.1-6, July 2016.

[14] Hao Rui, Du Huijing, "*Octagonal photonic crystal fiber dual-core polarization splitter*", Optiks, vol. 126, pp. 1415-1418, March 2015

[15] Jianhua Li, Rong Wang, Jingyuan Wang, Baofu Zhang, Zhiyoung Xu, Huali Wang, "*Novel magnetic field sensor based on magnetic fluids infiltrated dual-core photonic crystal fibers"*, Optical fiber technology, vol. 20, pp. 100-105, January 2014.

[16] D.C. Tee, N. Tamchek, and C.H.R. Ooi, "*Numerical Modeling of the Fundamental Characteristics of ZBLEN Photonic Crystal Fiber for Communication in 2-3* μm *Midinfrared Region*", An IEEE Photonics Society Publication, vol. 8, no. 2, pp. 1943-0655, April 2016.

[17] R. R. Mahmud, S. M. A. Razzak, and M. I. Hasan, "*A new photonic crystal fiber design on the high negative ultra-flattened dispersion for both X and Y polarization modes*", Optik, vol. 127, no. 20, pp. 8670-8677, June 2016.

[18] W. Cai, E. Liu, and B. Feng, *"Dispersion properties of a photonic quasi-crystal fiber with double cladding air holes*", Optik, vol. 127, no. 20, pp. 4438-4442, January 18, 2016.